Inverse Gas Chromatography with Film Cell Unit: An Attractive Alternative Method to Characterize Surface Properties of Thin Films

Géraldine L. Klein, Pierre G, Marie-Noëlle Bellon-Fontaine, Marianne Graber

1 **Inverse Gas Chromatography with film cell unit: an attractive alternative method to**

2 **characterize surface properties of thin films.**

3

4 Klein, G.L.[1], Pierre, G.[1], Bellon-Fontaine, M.N.[2], Graber, M.[1*]

5

6 (1) UMR 7266 CNRS - ULR LIENSs, Equipe Approches Moléculaires Environnement Santé. Université de La

7 Rochelle, UFR Sciences, Bâtiment Marie Curie, avenue Michel Crépeau, 17042 La Rochelle, France.

8 (2) UMR 0763 – MICALIS - Agro-ParisTech-INRA – Equipe Bioadhésion-Biofilm et Hygiène des Matériaux, 25

9 avenue de la république, 91300 Massy, France.

10 *corresponding author, email : mgraber@univ-lr.fr, tel: +33 5 46 45 86 30, fax: +33 5 46 45 82 65

11

12

Abstract

Inverse gas chromatography (IGC) is widely used for the characterization of surfaces. The present work describes a novel IGC tool, the recently developed film cell module, which measures monolithic thin solid film surface properties, whereas only samples in powder or fiber state or polymer-coated supports can be studied by classic IGC. The surface energy of four different solid supports was measured using both classic IGC with columns packed with samples in the powder state, and IGC with the new film cell module or the sessile drop technique, using samples in the film state. The total surface energy and its dispersive and specific components, were measured for Glass, Polyethylene, Polyamide and Polytetrafluoroethylene. Similar results were obtained for the four materials using the three different techniques. The main conclusion is that the new film cell module for IGC is an attractive alternative to the sessile drop technique as it gives very accurate and reproducible results for surface energy components, with significant savings in time and the possible control of sample humidity and temperature. This film cell module for IGC extends the application field of IGC to any thin solid film and can be used to study the effect of any surface treatment on surface energy.

Introduction

Surface energy measurements are very frequently used in material sciences to investigate wettability, adhesion characteristics, specific interactions with other molecules, cohesion and coating performance [1]. The most commonly used method to achieve such measurements is the Sessile Drop Technique using a goniometer which is relatively easy to perform and inexpensive. It consists of producing a drop of liquid on a solid and measuring the angle formed between the solid/liquid interface and the liquid/vapor interface, which is called the "contact angle" (CA) [2]. This angle, measured for a minimum of three types of liquids, and the known surface energy of the liquids are the parameters that are used to calculate the surface energy of the solid sample [3]. The main disadvantage of this method is that it is unable to reflect the totality of the surface energy properties, even if multiple droplets are deposited on various locations on the sample. CA gives reproducible results, but problems of reproducibility and accuracy may occur, in case of droplets that are not axially symmetric, or with surface-accessible pores, which can decrease the droplet volume by capillary action during measurement [4,5]. To overcome these disadvantages, alternative methods of measuring surface energy must be developed. Two of the most common alternative methods are capillary intrusion of liquid analytes into the sample and analyte adsorption onto a sample bed at infinite dilution using Inverse Gas Chromatography (IGC). Capillary intrusion and conventional IGC are both restricted to the samples in the powder or fiber state and also to polymers and polymer-

43   coated supports, either packed in columns or deposited as a film on the inside of a column to create a capillary column.

44   Nevertheless, a significant advance has been made recently with the development of a new system called film cell

45   module for IGC, which is convenient for flat and monolithic samples. That is why we chose to focus on this last method

46   as an alternative to CA measurements.

47   IGC is a vapor adsorption technique, which consists in an inversion of conventional gas chromatography. Physico-

48   chemical characteristics in the stationary phase are studied by injecting specific well-characterized gaseous probes [6-

49   8]. IGC is conventionally performed in columns containing the packed solid under investigation in the powder or fiber

50   state. The interaction between these probes and the solid material forming the stationary phase is then investigated by

51   determining the retention time for a given probe and used to calculate many physico-chemical properties, such as

52   surface energies of solids [9], enthalpy and entropy adsorption [10], solubility parameter, crystallinity [11], surface

53   heterogeneity [12], nanorugosity [11], glass transition [11] and melting temperature [7].

54   For surface energy determination, IGC presents many advantages compared to CA measurements: (i) the ability to

55   quantify strong interaction occurring between the solid and the probes that cannot be characterized by contact angle

56   measurement because of a contact angle close to zero [11], (ii) no problem of nanorugosity and surface heterogeneity

57   [13,14], as the interactions of the probes are measured all along a wide solid surface and give mean values of interaction

58   through the measure of the retention times, whereas CA measurements are restricted to the number of droplets

59   deposited on the surface. Film cell module for IGC provides quite a large interacting area with gaseous probes: a

60   relatively large rectangular sheet of flat sample (10 x 400 mm) is submitted to a gaseous flow carrying the probes,

61   which are situated in a small groove all along the sample (iii) IGC is less time consuming, (iv) IGC is an accurate,

62   versatile, reproducible method, with relatively easy sample preparation, (v) advanced IGC instruments have been

63   developed with fully automated operation, humidity and temperature control, *in-situ* sample preconditioning; thus

64   experiments may be carried out over appreciable temperature ranges, so that the temperature dependence of

65   thermodynamic interactions can be determined.

66   The field of application of conventional IGC is wide. It concerns materials in the powder or fiber state and also

67   polymers, that are either coated onto inert support and packed into columns or deposited as a uniform film on the inside

68   of a column to create a capillary column [15]. It includes synthetic and biological polymers [8], paper and other

69   cellulosics, fillers and pigments, flavourings and perfumes, minerals and inorganic materials [16], food products [17],

70   packaging and coatings, pharmaceuticals and medical products [18], building materials, cosmetics and ingredients,

71   natural and artificial fibers [19], supported catalysts and microporous material [20] and adsorbents [21]. The new film

72   cell module for IGC is able to extend these different application fields to monolithic thin solid films.

73   In the present work, we compare three approaches to determine the surface energy of solids, including the dispersive

74 and specific components: (i) conventional IGC at infinite dilution (IGC-C) with solid samples in the powder state

75 packed in a column as a fixed bed, (ii) two-dimension IGC with the film cell module at infinite dilution (IGC-FC) with

76 solid samples in the film state and (iii) analysis of CA data using the Good-van Oss theory, with solid samples in the

77 film state. The surface energetics of four different materials including polymers (Polyamide (PA),

78 Polytetrafluoroehylene (PTFE), and Polyethylene (PE) and glass were determined. These materials all exist in both

79 powder and film states and their surface energy was investigated by the three IGC-C methods for powders and by IGC-

80 FC and CA for films.

81 To our knowledge, no study has yet been devoted to the comparison of surface energy obtained for the same material in

82 the granular state using IGC-C columns and in the film state using IGC-FC, nor to the comparison of surface energy

83 values obtained by IGC-FC and CA for samples in the film state.

84

85 **Experimental**

86 All materials (powders or films) were washed as below. The sample was immersed in PCC-54 (Fisher Scientifics) 2 %

87 (v/v) for 10 minutes with an orbital agitation (100 rpm, Heidolph Rotamax 120). Then they were rinsed five times with

88 sterile ultrapure water at 40°C for 5 minutes with the same orbital agitation. Each film sample was finally wiped with

89 optical cleaning tissue (Whatman 105), and was dried at 40°C into an incubator. All samples were stored at room

90 temperature.

91 For CA measurements, a minimum of 10 droplets were measured on each surface.

92 All experiments involving IGC analysis were performed in triplicate, so a standard deviation can be calculated.

93

94 **Instrumentation and Reagents**

95 CA were measured with a goniometer G40 (Krüss, Germany) at room temperature (23°C) with an accuracy of ± 2°C.

96 The chromatographic experiments were performed using an IGC 2000 (Surface Measurement Systems, London, UK). A

97 technical drawing of the Film-cell module for IGC-FC (Surface Measurement Systems, London, UK) is presented in

98 Figure 1. As an external bench-top unit made from stainless steel material, the film cell module provides an interacting

99 area of 350 x 40 mm with a 0.3 mm groove.

100 The apolar probes (decane (C10), nonane (C9), octane (C8), heptane (C7) and hexane (C6)) and polar probes

101 (dichloromethane, chloroform, ethyl acetate, toluene, diiodomethane and formamide) were supplied by Sigma with

102 HPLC purity. They were used without further purifications. Ultrapure water was obtained via a Milli Q system

103 (Millipore, France). The relevant characteristics of both amphotheric and polar probes, including the molecular cross-

104 sectional surface area, the acid-base character and the surface energy components are presented in Table I.

105 Contact angle (CA), IGC-C and IGC-FC measurements were performed on four different supports: Glass (Thermo,

106 1mm thick), Polyethylene (PE, Goodfellow 0.5mm thick), Polyamide-nylon 6 (PA, Goodfellow 0.5 mm thick) and

107 Polytetrafluoroethylene (PTFE, Goodfellow 0.5 mm thick). For measuremenst by IGC-FC, the film materials was cut in

108 10 x 400 mm pieces, whereas IGC-C measurements in packed column were performed with the powders with particle

109 size ranging from 100 to 150 µm of diameter. Packing is accomplished with the aid of a mechanical vibrator. For PE,

110 PA and PTFE, both powder and film had the same chemical composition. Both powder or film glass samples were made

111 in soda-lime-silica glass.

112

113 **Methods**

114 ***Determination of surface energy by CA***

115 According to the GVOC (Good Van Oss Chaudhury) approach [3], CA were converted into surface energy components

116 using the Young-van Oss equation (Eq.1), which ignores spreading pressure and highlights Lifshitz-van der Waals and

117 Lewis acid/base surface free energy components.

118 $$\gamma_L^t \left(1 + \cos\theta\right) = 2\left(\sqrt{\gamma_S^{LW}\gamma_L^{LW}} + \sqrt{\gamma_S^+\gamma_L^-} + \sqrt{\gamma_S^-\gamma_L^+}\right) \qquad (1)$$

119 Here, γ^t, γ^{LW}, γ^+ and γ^- are the total surface energy, Lifshitz-van der Waals, electron-acceptor (or Lewis-acid) and

120 electron-donor (or Lewis-base) components of the surface free energy respectively; θ is the CA and the subscripts L and

121 S denote the liquid and solid samples, respectively.

122 Equation 2 allowed accessing to the Lewis acid-base components of the surface energy:

123 $$\gamma^{AB} = 2\sqrt{\gamma^+\gamma^-} \qquad (2)$$

124

125 ***Determination of surface energy by IGC***

126 IGC was operated at "infinite dilution.

127   *Determination of the net retention volume*

128 The net retention volume V_N of vapor probes is then calculated using Eq.3 [22]:

129 $$V_N = j \times t_N \times F \text{ (ml)} \qquad (3)$$

130 where t_N is the net retention time, calculated using Eq. (4); F (ml.min^{-1}) the carrier gas flow rate, at the sample

131 temperature and j is the James and Martin compressibility factor, calculated using Eq. (5), taking into account the

132 compression of the gas and the pressure drop upstream the column or module [23].

133 $t_N = t_R - t_0$ (4)

134 where t_R is the experimental retention time used by a probe to cross the column or the film cell and t_0 the dead time of

135 the column or film cell, determined through the injection of methane which does not adsorb on the solid.

136 $j = \frac{3}{2} \times \frac{(P_i / P_0)^2 - 1}{(P_i / P_0)^3 - 1}$ (5)

137 where P_i and P_0 are the inlet and outlet pressures respectively.

138 In practice, j is considered to be equal to 1 when using the film cell module.

139 *Determination of the free energy of adsorption*

140 The net retention volume V_N of vapor probes is directly related to the variation of the free energy of adsorption ΔG_{ads},

141 according to Eq.6

142 $\Delta G_{ads} = -(R \times T \times \ln V_N) + C$ (6)

143 where C is a constant depending on the choice of a reference state of the adsorbed probe and also on the total area of the

144 solid accessible to the probe, R is the gas constant and T the absolute temperature. ΔG_{ads} takes into account two kinds of

145 interactions (Eq.7): dispersive interactions ΔG_{ads}^D, corresponding to London forces and specific interactions ΔG_{ads}^{SP},

146 which consists mostly out in Lewis acid-base contributions.

147 $\Delta G_{ads} = \Delta G_{ads}^D + \Delta G_{ads}^{SP}$ (7)

148 To obtain the dispersive as well as the specific parts of ΔG_{ads}, different apolar and polar vapor molecules respectively

149 are injected and their net retention volume V_N determined.

150 *Determination of the dispersive component of the surface energy*

151 In case of apolar probes, like n-alkanes, which can only interact by dispersive interactions, V_N is related to ΔG_{ads}^D by

152 Eq.8, which uses the relation of Fowkes [24]:

153 $\Delta G_{ads}^D = -R \times T \times \ln V_N + C = -2N_A (\gamma_S^D)^{\frac{1}{2}} \times a \times (\gamma_L^D)^{\frac{1}{2}} + C'$ (8)

154 where N_A is the Avogadro constant, R the gas constant, a the molecular cross-sectional area of probes adsorbing on the

155 solid surfaces (m^2) and γ_L^D the dispersive component of the liquid probe surface energy and γ_S^D the dispersive

156   component of the surface energy of the solid. If a series of alkanes is injected, γ_S^D can be derived from the slope of the

157   fitted line, which is called the "alkane line" in a plot of $RTlnV_N$ versus $a\left(\gamma_L^D\right)^{\frac{1}{2}}$.

158   *Determination of the specific component of the surface energy*

159   The experimental points for the polar probe molecules are located above the alkane line in the surface energy plot. The

160   vertical distance between each point and the alkane straight line represents the specific contribution of the interaction,

161   which is expressed as the specific free energy ΔG_{ads}^{SP} .

162   On the whole, this approach for acid-base calculations used in IGC is the van Oss concept, which provides acid and

163   base numbers in the same units as the dispersive surface energy, according to Eq.9:

164      $$\Delta G_{ads}^{SP} = 2 \times N_a \times a \times \left(\left(\gamma_L^+ \times \gamma_S^-\right)^{\frac{1}{2}} + \left(\gamma_L^- \times \gamma_S^+\right)^{\frac{1}{2}} \right) \quad (9)$$

165   where ΔG_{ads}^{SP} is the specific component of the surface energy (mJ/mol), N_A is the Avogadro constant, a the molecular

166   cross-sectional area of adsorbates (m²), γ_L^+ and γ_L^- (mJ/m²) the electron acceptor (acid) and electron donor (base)

167   parameters of the probe molecule, γ_S^+ and γ_S^- (mJ/m²) the electron acceptor (acid) and electron donor (base)

168   parameters of the surface. Then γ_S^+ and γ_S^- can be calculated thanks to two couples of complementary polar probes:

169   dichloromethane (DCM)/ethyl acetate (EA) and toluene (T)/chloroform (CF), where γ_S^- is equal to zero for DCM and

170   CF and γ_S^+ is equal to zero for EA and T.

171   The specific or polar component of surface energy γ_S^{SP} (mJ/m²) can then be calculated from the γ_S^+ and γ_S^- according

172   to the Eq. 10. Finally, the total surface energy γ_S^t is also accessible through the Eq. 11.

173      $$\gamma_S^{SP} = 2 \times \sqrt{\gamma_S^- \times \gamma_S^+} \quad (10)$$

174      $$\gamma_S^t = \gamma_S^{SP} + \gamma_S^D \quad (11)$$

175

176   A conditioning period of 12 hours was applied for each experiment to equilibrate the chromatographic column or the

177   module with their sample *in situ* at constant conditions of temperature (40°C) and gas flow (helium, 10 mL/min) with a

178   relative humidity (RH) of zero, except when the effect of RH on surface energy was studied. In this case RH was equal

179   to values ranging from 10 to 50% in the carrier gas. The optimal quantity of probes to obtain an infinite dilution mode

180   and sharp and symmetrical peaks were obtained at $p/p_0 = 0.025$, with p being the partial pressure of the solute in the gas

181   phase and p_0 the saturation vapor pressure of the solute.

182

183

184   **Results**

185   *Comparison of the surface energy obtained for materials in either the granular state using IGC-C columns or in the*

186   *film state using IGC-FC*

187   The main aim of this paper is to investigate the use of a new system called film cell module for IGC, to study the

188   surface energetics of flat and monolithic samples. In order to assess whether meaningful data were obtained using this

189   new module, the surface energetics of the same materials in either the granular state or in the film state were assessed by

190   using respectively IGC-C and IGC-FC.

191   The IGC-FC method allows direct access to the surface energy of solid films. However, the use of the film cell module,

192   which is made of stainless steel (Figure 1), leads to a measurement bias because it is not inert. The empty module has a

193   significant polar component for its surface energy that must be substracted by performing a blank. The dispersive

194   component is, however, negligible. In contrast, IGC-C columns are made of inert glass and a blank is not necessary.

195   The results from both IGC-FC and IGC-C are summarized in Table II; the values of the total surface energy calculated

196   from the IGC-FC experiments are in good agreement with those calculated from IGC-C for the different tested supports,

197   except for PA. For this material, these values are equal to 43.8±1.8 mJ/m^2 from IGC-C and 48.5±2.3 mJ/m^2 from IGC-

198   FC, respectively. The magnitude of all values determined here for all materials compared reasonably well with

199   previously reported values in the literature [25].

200   For all the surface energy components measured in IGC-FC the calculated values are not significantly different from

201   those obtained in IGC-C (Table II), except for PA and for the electron-donor component of glass. For PA, both

202   dispersive and specific components of surface energy obtained from IGC-FC were higher than the ones obtained from

203   IGC-C. For glass, the electron-donor component from IGC-C was higher than from IGC-FC.

204   *Comparison of the surface energy obtained by IGC-FC and CA for materials in the film state*

205   CA is one of the most commonly used techniques in the characterization of surface energetics and wettability of

206   materials in the film state. It was therefore used as a point of comparison with IGC-FC.As observed in Table II, the

207   values of the total surface energy calculated from the CA experiments corroborate the surface energy trends established

208   with IGC-FC and give somewhat lower absolute values for these numbers, in case of the three substrata with the lowest

209 surface energy: PTFE, PE and PA. A GVOC approach was used for CA experiments, which allows the conversionof CA

210 into γ_S^{LW} (Lifshitz-van der Waals), and γ_S^+ and γ_S^- (Lewis acid and base) surface energy components. It is recognized

211 that the Lifshitz-van der Waals contribution is primarily due to dispersion forces or London interactions, although small

212 contributions resulting from the presence of permanent dipoles may also be accounted for in this term (induction or

213 Debye and orientation or Keesom interactions) [26]. Therefore, it is relevant to compare values obtained from CA and

214 values obtained from IGC-FC.

215 For PTFE, PE and PA, the γ_S^D obtained using IGC-FC were slightly superior to the γ_S^{LW} values obtained from CA:

216 Interestingly, in the case of glass, a higher value for the total surface energy (γ_S^t = 56.2 ± 0.3 mJ/m²) was calculated

217 with CA measurements, compared to IGC-FC, for which a value of 47.9 ± 3.3 mJ/m² was obtained (Table II). This

218 difference is statistically significant with a *p-value* of 0.00021 (calculated from Student test). It arose only from the γ_S^-

219 values that are equal to 11.0 ± 2.6 mJ/m² with IGC-FC and 54.1 ± 2.6 mJ/m² with CA, whereas γ_S^D and γ_S^{LW} values on

220 the one side and γ_S^+ values on the other side were very similar.

221

222 ***Effect of relative humidity on the surface energy of glass measured by IGC-FC***

223 The influence of the relative humidity (RH) on the evolution of the specific component of the surface energy for glass

224 was examined using IGC-FC.

225 The results for the total surface energy and its different components measured by IGC-FC as a function of RH are

226 presented in Figure 2. On the right of Figure 2 are also presented the results for the total surface energy and its different

227 components for glass measured by CA with atmospheric RH equal to 50%. For glass from IGC-FC measurements, it

228 appears that the electron-donor component significantly increases with the RH. On the other hand, the dispersive and

229 electron-acceptor components maintain similar values all along the humidity gradient. The values calculated for the

230 electron-donor component increased from 11.0 mJ/m² to 66.79 mJ/m² in accord with the gradient of RH in the gaseous

231 stream and from 0 to 50 %RH in IGC-FC, and showed a linear tendency between 10 and 50 %RH, with a slope equal to

232 15.3 $(mJ/m^2)/(\%RH)$. The increase in the electron-donor component with RH may be due to the interaction of the

233 probes with water molecules adsorbed on the surface and the formation of silanol (Si-O-H) sites by chemisorption. For

234 glass from CA measurements taken at room temperature with atmospheric RH equal to 50%, it appears that the value of

235 the electron-donor component is close to the one obtained with IGC-FC at 30 and 40%RH.

236

237

238 **Discussion**

239 As mentioned in the results part, the values obtained for surface energetics by IGC-FC corroborate those surface energy

240 trends established with IGC-C and the magnitude of these numbers compare reasonably well. Some significant

241 differences between the two methods exist however for the absolute values of both dispersive and specific components

242 of surface energy found for PA and also for the electron-donor component of glass. These differences may arise from an

243 effect of the geometry of the materials on the interpreted surface energetics, as shown previously for different works

244 using IGC. For example, Guillet et al. reported differences for polystyrene between studies using pure polymer packed

245 in a column and or capillary columns coated on the inside with polymer [15]. They found that specific retention volume

246 values were slightly higher for an open column than for a packed column, possibly because of the higher specific

247 surface area available in the open column. Jones et al. mention that milling increased the dispersive surface energy and

248 surface acidity of lactose and several respiratory drugs. These effects could be ascribed to the introduction of surface

249 structural defects or to the disruption of particle flaws exposing surfaces rich in hydroxyl groups in the case of lactose

250 [18].

251 The differences between results from CA and IGC are well known and the discussion about this point is out of the scope

252 of this paper. These differences arise from the vastly different energetics between the two systems, involving

253 gas/condensed phase interaction for IGC and condensed phase/condensed phase interaction for CA. In the present study,

254 another difference was introduced between the two systems through the difference in RH values during experiments:

255 RH was not controlled during CA experiments and was equal to the ambient atmospheric RH which was 50% that day.

256 This is one of the reasons explaining the important difference in the γ_S^- values found for glass using CA or IGC at RH

257 equal to 0. Glass is by far the most hydrophilic material among the four studied. It is composed mainly of silica, and

258 previous studies have shown that water can rupture siloxane (Si-O-Si) bonds via dissociative chemisorption, forming

259 silanol (Si-O-H) sites, in particular at the first stage of humidification [27,28]. This chemical change occurring at the

260 surface of glass also affects the specific component of the surface energy. For this reason, the effect of RH on the

261 surface energy was studied for glass by IGC-FC. It appears that when increasing the RH from 0 to 50% in IGC, the

262 difference in the γ_S^- values found for glass using CA or IGC-FC decreases. However, considering that temperature is

263 changed from 23°C to 40°C between CA and IGC-FC experiments, the quantity of adsorbed water on glass for a same

264 RH is higher in case of IGC-FC, undercutting the relevance of the exact comparison of results from CA and IGC-FC at

265 the same RH.

266

Conclusion

The new film cell module for inverse Gas Chromatography experiments, presented in this work, enables to obtain meaningful data for the surface energetics of flat and monolithic samples, for solid materials with varying surface properties: PTFE, PE, PA and glass. In comparison with CA measurements, it offers the possibility to control the temperature and the RH perfectly during automated and rapid experiments, including *in situ* conditioning.

Thanks to these preliminary results, it can be concluded that IGC-FC appears as a viable method. However, more extensive study is needed to identify the origin of differences with standard IGC-C, since the differences in surface geometry may also have an influence on the interpreted surface energetics. IGC-FC extends the possibility of IGC to flat and monolithic samples. The analysis can be performed directly on two dimensions samples, without any prior preparation. The field of application of IGC-FC is large and includes the easy analysis of the influence of cleaning or painting on the surface energy parameters of solid surfaces, important in a wide variety of industries.

278

284

References

[1] Good, R.J.; Contact-angle, wetting and adhesion – A critical review; *Journal of Adhesion Science Technolology*, (1992); 6:1269-1302.

[2] Zisman, W.A.; Fowkes, F.M. (ed.) Contact Angle, Wettability and Adhesion, Advances in Chemistry Series, Vol. 43, American Chemical Society, Washington D.C., (1964).

[3] van Oss, C.J., Chaudhury, M.K., Good, R.J.; Interfacial Lifshitz-van der Waals and polar interactions in macroscopic systems; *Chemical Reviews*, (1988); 88:927-941.

[4] Chini, S.F., Amirfazhi, A. ; A method for measuring contact angle of asymetric and symetric drops ; *Colloïds and Surfaces A: Physicochemical and Engineering Aspects*, (2011); 388: 29-37.

[5] Wenzel, R.N.; Surface roughness and contact angle; *Journal of Physical and Colloid Chemistry*, (1949); 53:1466-1467.
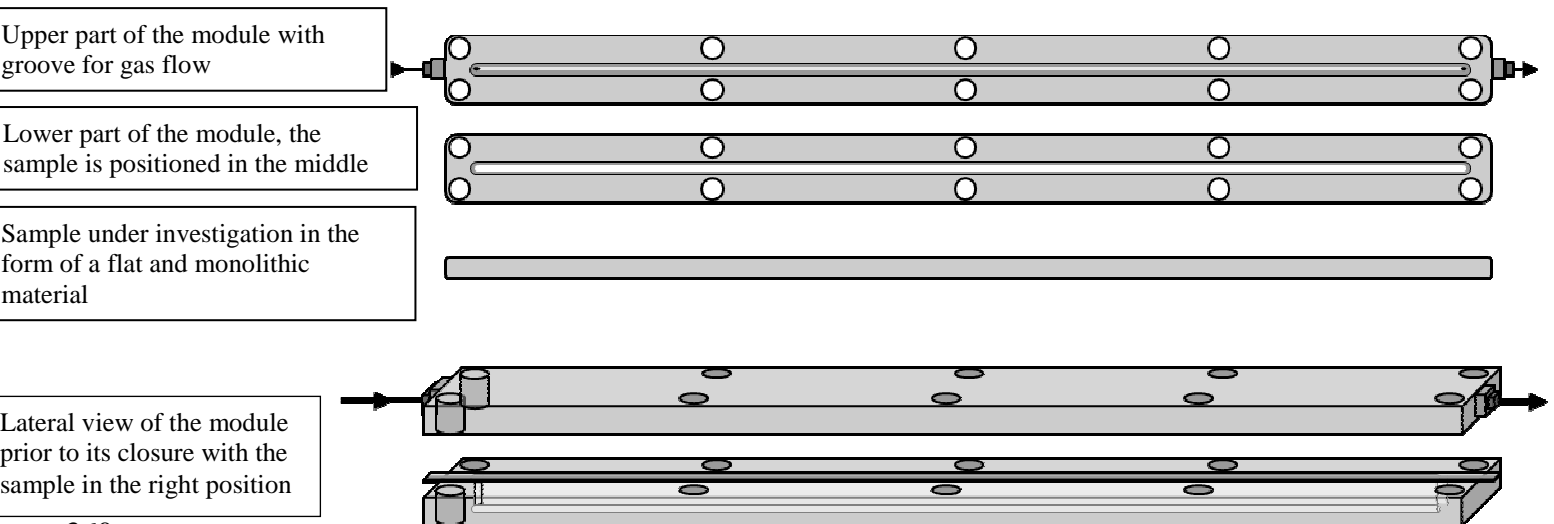
[6] Conder, J.R., Young, C.L.; Wiley, J. & Sons (ed). Physical measurements by gas chromatography, Whiley-

297   interscience, New-York, (1969).

298   [7] Hegedus, C.R., Kamel, I.L.; A review of inverse gas chromatography theory used in the thermodynamic analysis of

299   pigment and polymer surfaces; *Journal of Coatings Technology*, (1993); 65:23-30.

300   [8] Voelkel, A.; Inverse gas chromatography: characterization of polymers, fibers, modified silicas, and surfacants;

301   *Critical Reviews in Analytical Chemistry*, (1991); 22: 411-439.

302   [9] Huang, X., Shi, B., Li, B., Li, L., Zhang, X., Zhao, S.; Surface characterization of nylon 66 by inverse gas

303   chromatography and contact angle; *Polymer Testing*, (2006); 25:970-974.

304   [10] Santos, J.M.R.C.A., Fagelman, K., Guthrie, J.T.; Characterisation of the surface Lewis acid-base properties of

305   poly(butylene terephthalate) by inverse gas chromatography; *Journal of Chromatography A*, (2002); 969:111-118.

306   [11] Santos, J.M.R.C.A., Guthrie, J.T.; Analysis of Interactions in Multicomponent Polymeric Systems: The Key-role of

307   Inverse Gas Chromatography; *Materials Science and Engineering Reports*, (2005); 50:79-81.

308   [12] Gavril, D., Nieuwenhuys, B.E.; Investigation of the surface heterogeneity of solids from reversed-flow inverse gas

309   chromatography; *Journal of Chromatography A*, (2004); 1045:161-172.

310   [13] Brendlé, E., Papirer, E.; A new topological index for molecular probes used in inverse gas chromatography for the

311   surface nanorugosity evaluation, 1. Method of evaluation; Journal of Colloid and Interface Science, (1997a); 194:207-

312   216.

313   [14] Brendlé, E., Papirer, E.; A new topological index for molecular probes used in inverse gas chromatography, 2.

314   Application for the evaluation of the solid surface specific interaction potential; Journal of Colloid and Interface

315   Science, (1997b); 194:217-224.

316   [15] Guillet,J.E., Romansky, M., Price, G.J., van der Mark, R.; Studies of Polymer Structure and Interactions by

317   Automated Inverse Gas Chromatography. In Inverse Gas Chromatography, Characterization of Polymers and Other

318   Materials, Chapter 3. ACS symposium Series 391, American Chemical Society: Washington, DC, (1989), pp. 20-32.

319   [16] Papirer, E., Brendlé, E., Ozil, F., Balard, H.; Comparison of the surface properties of graphite, carbon black and

320   fullerene samples, measured by inverse gas chromatography; *CARBON*, (1999); 7:1265-1274.

321   [17] Boutboul, A., Giampaoli, P., Feigenbaum, A., Ducruet, V.; Influence of the nature and treatment of starch on aroma

322   retention; *Carbohydrate Research*, (2002); 47:73-82.

323   [18] Jones, M.D., Young, P., Traini, D.; The use of inverse gas chromatography for the study of lactose and

324   pharmaceutical materials used in dry powder inhalers; *Advanced Drug Delivery Reviews*, (2012); 64:285-293.

325   [19] Vega, A., Diez, F.V., Hurtado, P., Coca, J.; Characterization of polyarylamide fibers by inverse gas

326   chromatography; *Journal of Chromatography A*, (2002); 962:153-160.

327   [20] Marton, Z., Chaput, L., Pierre, G., Graber, M.; Lipase hydration in the gas phase: Sorption isotherm measurements

and inverse gas chromatography; *Biotechnology Journal*, (2010); 5:1216-1225.

[21] Elizalde-Gonzalez, M.P., Ruiz-Palma, R.; Gas chromatographic characterization of the adsorption properties of the natural adsorbent CACMM2; *Journal of Chromatography A*, (1999); 845:373-379.

[22] Schultz, J., Lavielle, L., Martin, C.; Surface properties of carbon-fibers determined by inverse gas chromatography; *Journal of Chemical Physics*, (1987); 84:231-237.

[23] James, A.T., Martin, J.P.; Gas-liquid partition chromatography: the separation and micro-estimation of volatile fatty acids from formic acid to dodecanoic acid; *Biochemical Journal*, (1952); 50:679-690.

[24] Fowkes, F.M.; Additivity of intermolecular forces at interfaces. 1. Determination of contribution to surface and interfacial tensions of dispersion forces in various liquids; *Journal of Physical Chemistry*, (1963); 67:2538-2541.

[25] Kinloch, A.J.; Adhesion and Adhesives: Science and Technology, Chapman and Hall, London, (1987).

[26] Steele, D.F., Moreton, R.C., Staniforth, J.N., Young, P.M., Tobyn, M.J., Edge, S.; Surface Energy of Microcrystalline Cellulose Determined by Capillary Intrusion and Inverse Gas Chromatography; *The AAPS Journal*, (2008); 10:494-503.

[27] Sun, C., Berg, J.C.; Effect of moisture on the surface free energy and acid-base properties of mineral oxides; *Journal of Chromatography A*, (2002); 969:59-72.

[28] Mahadevan, T.S., Garofalini, S.H.; Dissociative Chemisorption of Water onto Silica Surfaces and Formation of Hydronium Ions; *The Journal of Physical Chemistry C*, (2008); 112:1507-1515.

[29] Hefer, A.W., Little, D.N., Herbert, B.E.; Bitumen surface energy characterization by inverse gas chromatography; *Journal of Testing and Evaluation*, (2007); 35:233-239.

[30] Della Volpe, C., Siboni, S.; Some reflections on acid-base solid surface free energy theories; *Journal of Colloid and Interface Science*, (1997); 195:121-136.

[31] Schultz, J., Tsutsumi, K., Donnet, J.B.; Surface properties of high-energy solids I. Determination of the dispersive component of the surface free energy of mica and its energy of adhesion to water and n-alkanes; *Journal of Colloid and Interface Science*, (1977); 59:272-276.

[32] van Oss, C.J., Chaudhury, M.K., Good, R.J.; Monopolar surfaces; *Advances in Colloid and Interface Science*, (1987); 28:35-64.

[33] van Oss, C.J., Giese, R.F., Li, Z., Murphy, K., Norris, J., Chaudhury, M.K., Good, R.J.; Determination of contact angles and pore sizes of porous media by column and thin layer wicking; *Journal of Adhesion Science Technology*, (1992); 6:413-428.

358   Figure 1: Technical drawing of the film cell module for iGC (35x400x11 mm). The arrows show gas flow.

359

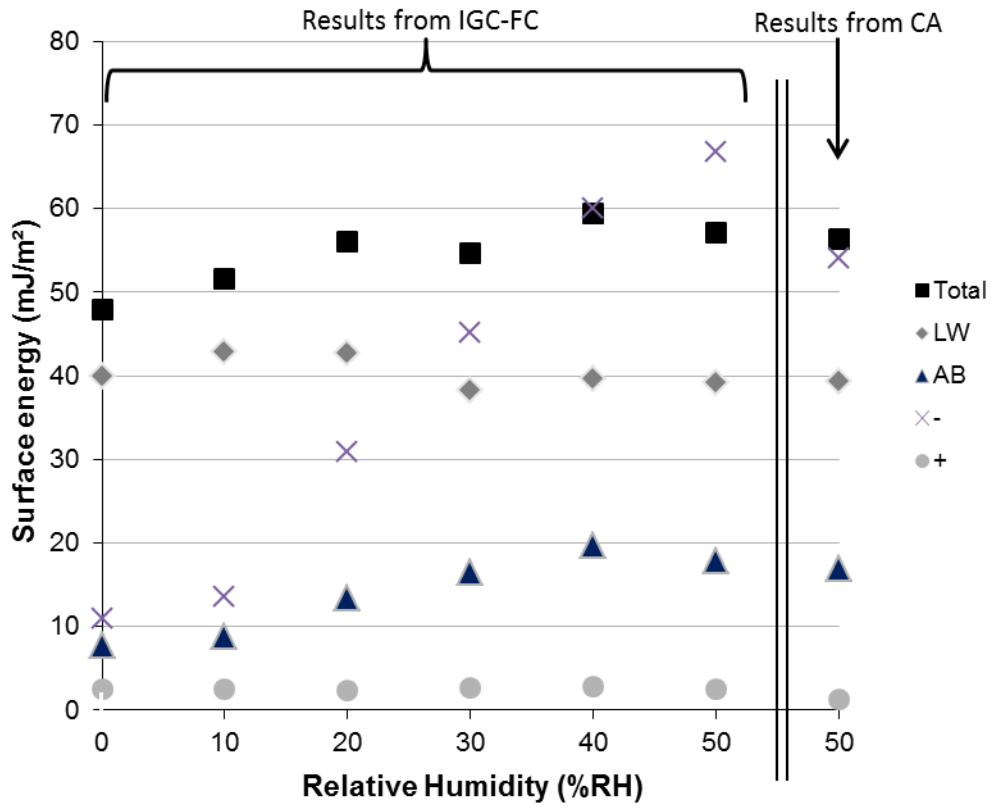| Upper part of the module with groove for gas flow |
| Lower part of the module, the sample is positioned in the middle |
| Sample under investigation in the form of a flat and monolithic material |
| Lateral view of the module prior to its closure with the sample in the right position |

360
361

362

363 Figure 2: Surface energy components measured on Glass, depending on a RH gradient established into the film cell
364 module during iGC experiments and values obtained with CA measurements at "ambient" RH.

365

366
367

368   Table I: Acid-base character and values of cross sectional area and surface energy components of amphoteric and polar

369   probes used in contact angle and IGC experiments. Values from [29-33], DCM = dichloromethane, EA = ethyl acetate,

370   T = toluene, CF = chloroform.

Solvents - probes	Molecular cross-sectional surface area "a" (m^2)	Surface energy (mJ/m^2) of the liquid probes			
		total surface energy γ_L^t	dispersive component γ_L^D	electron acceptor parameter γ_L^+	electron donor parameter γ_L^-
n-alkanes					
C6	5.15 x10^{-19}	18.4	18.4	0.0	0.0
C7	5.73 x10^{-19}	20.3	20.3	0.0	0.0
C8	6.30 x10^{-19}	21.3	21.3	0.0	0.0
C9	6.92 x10^{-19}	22.7	22.7	0.0	0.0
C10	7.44 x10^{-19}	23.9	23.9	0.0	0.0
Contact angle					
water	/	72.8	21.8	25.5	25.5
formamide	/	58.0	35.6	2.3	39.6
diiodomethane	/	50.8	50.8	0.0	0.0
iGC					
DCM	2.99 x10^{-19}	26.5	26.5	5.2	0.0
EA	3.29 x10^{-19}	23.9	23.9	0.0	19.2
T	4.20 x10^{-19}	28.5	28.5	0.0	2.3
CF	3.51 x10^{-19}	27.2	27.2	3.8	0.0

371

Table II: Calculated values of surface energy for five materials, PA = polyamide-6, PE = polyethylene, PTFE = polytetrafluoroethylene and Glass. [a] Materials at powder state. [b] Materials at film state. Standard deviations were calculated with n ≥ 10 measurements.

Materials	γ_S^t (mJ/m^2)	γ_S^{LW} (mJ/m^2) (CA) γ_S^D (mJ/m^2) (iGC)	γ_S^{SP} (mJ/m^2)	γ_S^+ (mJ/m^2)	γ_S^- (mJ/m^2)
iGC columns[a] (iGC-C)					
PTFE	19.5 ± 2.3	19.1 ± 2.3	0.4 ± 0.0	0.1 ± 0.0	0.5 ± 0.1
PE	32.2 ± 2.1	31.6 ± 2.1	0.6 ± 0.0	0.1 ± 0.0	0.9 ± 0.2
PA	43.8 ± 1.8	41.9 ± 1.7	1.9 ± 0.2	0.2 ± 0.1	4.1 ± 2.5
Glass	46.7 ± 1.6	39.8 ± 1.8	7.0 ± 0.3	0.5 ± 0.2	22.8 ± 1.8
iGC film-cell[b] (iGC-FC)					
PTFE	21.1 ± 3.1	21.0 ± 3.2	0.1 ± 0.1	0.0 ± 0.0	0.5 ± 0.3
PE	32.9 ± 1.5	31.0 ± 1.5	1.9 ± 0.6	0.3 ± 0.3	2.7 ± 1.2
PA	48.5 ± 2.3	44.7 ± 2.6	3.8 ± 1.2	0.4 ± 0.3	8.9 ± 1.7
Glass	47.9 ± 3.3	40.0 ± 2.2	7.8 ± 1.1	2.5 ± 2.1	11.0 ± 2.6
Contact angle[b] (CA)					
PTFE	17.1 ± 0.9	15.9 ± 0.6	1.2 ± 0.3	0.2 ± 0.1	1.9 ± 0.5
PE	32.5 ± 2.7	29.3 ± 1.5	3.2 ± 1.2	0.8 ± 0.3	3.4 ± 1.6
PA	42.4 ± 0.9	40.4 ± 0.8	2.0 ± 0.2	0.1 ± 0.0	11.5 ± 1.5
Glass	56.2 ± 0.3	39.4 ± 1.6	16.8 ± 1.9	1.3 ± 0.3	54.1 ± 0.2